

**Thermodynamic characterization of temperature- and composition-dependent mixed micelle formation in aqueous medium**

Journal:	<i>Journal of Surfactants and Detergents</i>
Manuscript ID	JSD-17-0120.R1
Manuscript Type:	Original Article
Date Submitted by the Author:	12-Jul-2017
Complete List of Authors:	Juhász, Ádám; Department of Physical Chemistry and Materials Sciences Tabajdi, Réka; Department of Physical Chemistry and Materials Sciences Dékány, Imre; Department of Physical Chemistry and Materials Sciences Csapó, Edit; Department of Physical Chemistry and Materials Sciences ; MTA-SZTE Supramolecular and Nanostructured Materials Research Group
Keywords:	Non-ionic surfactants, Application of surfactants

# Thermodynamic Characterization of Temperature- and Composition-dependent Mixed Micelle Formation in Aqueous Medium

Ádám Juhász<sup>1,2</sup>, Réka Tabajdi<sup>1</sup>, Imre Dékány<sup>1</sup>, Edit Csapó<sup>1,2,\*</sup>

<sup>1</sup> Department of Physical Chemistry and Materials Sciences, University of Szeged, H-6720, Aradi v.t.1, Szeged, Hungary

<sup>2</sup> MTA-SZTE Biomimetic Systems Research Group, University of Szeged, H-6720 Dóm tér 8., Szeged, Hungary

\*Corresponding author: juhaszne.csapo.edit@med.u-szeged.hu

## Abstract

This article provides a detailed description of micellization of binary nonionic surfactant system (Lutensol AP9 and AP20) at different compositions and temperatures in aqueous medium. Critical micelle concentrations of the individual components ( $CMC_i$ ) and the mixed surfactants ( $CMC_m$ ) were determined via surface tension measurements in the temperature range of 288.15 - 318.15 K. Based on the magnitude and temperature dependence of CMC values the Gibbs energy- ( $\Delta_{mic}G$ ), enthalpy- ( $\Delta_{mic}H$ ), and entropy change ( $\Delta_{mic}S$ ) of micellization were evaluated. At 288.15 K the thermodynamic parameters were confirmed by isotherm titration calorimetry (ITC). Using the regular solution theory (RST), the compositions of the mixed micelles ( $X_M$ ) and molecular interaction parameters ( $\beta_M$ ) were estimated for all molar ratios and temperatures. The results of evaluations based on the closed association model and RST were compared.

**Keywords:** critical micellization concentration; excess Gibbs free energy; mixed micelles; nonionic surfactant; regular solution theory

## Introduction

Surface active **agents** or surfactants, as they are commonly known, are widely used chemicals in household detergents, personal care- and food products. Surfactants play an important role in these **applications** as stabilizing- emulsifying-, foaming agents and detergents. Nonylphenol ethoxylates (NPE) are the most widely used members of the larger alkylphenol ethoxylate family of nonionic surfactants. They are produced in large volumes resulting in widespread release to the aquatic environment. National environmental protection agencies and the detergent manufacturers have cooperated to reduce their utilization, but NPEs are still widely applied in large quantities in industrial cleaning applications.

The industrial use (food-, pharmaceutical-, petrochemical industry *etc.*) of mixed micelles of nonionic surfactants in aqueous solution is well-known [1–5]. When there are adequate synergistic interactions between the individual components of micelles, the CMC of the binary surfactant mixture can be lower and the binary mixed micelle is thermodynamically more stable than the single surfactant-containing micelle [6–9]. Deeper understanding of the origin of non-ideal and synergistic behavior may help to design more efficient surfactant mixtures in order to reduce the amount of chemicals used in industrial applications. Several research groups have published **reports** on mixed micelle formation [10, 11] and thermodynamic characterization of the micellization [12, 13], but only a few articles provide deeper information on the temperature [14] and composition [15] dependence of the CMC in mixed nonionic surfactant systems combining the advantages of both approach. The aim of this work was to characterize thermodynamically the binary nonionic surfactant mixture of octylphenol ethoxylate-9EO (AP9) and octylphenol ethoxylate-20EO (AP20) which has not been reported in the literature previously. Moreover, the other goal was also to compare the results of evaluations based on the closed association model theory and regular solution theory (RST).

## Theoretical background

The mechanism of micelle formation from individual surfactant molecules ( $S$ ) can be described by a series of step-wise equilibrium states:



with a series of equilibrium constants ( $K_n$ ) for  $n = 2 - \infty$ , and where the various thermodynamic parameters for the aggregation process can be expressed in terms of  $K_n$  [16]. According to the study of the micellization of surfactants, the determination of the CMC is crucial. Furthermore, two models are employed generally in the theoretical thermodynamic interpretation of micelles; (i) the phase separation model and (ii) the closed association model [17, 18]. The latter concept is often called the mass-action or closed-association model. Both methodologies require the **determination** of the CMC in order to determine important physicochemical properties (e.g. surface tension, conductivity, osmotic pressure etc.) as a function of surfactant concentration.

In the closed-association model, with the size range of spherical micelles around the CMC being very limited, it is assumed that only one of  $K_n$  value is dominant, and micelles and monomeric species are considered to be in chemical equilibrium:



where  $n$  the number of surfactant molecules,  $S$ , associating to form the micelle (i.e., the aggregation number). This model assumes a dissociation–association equilibrium between solvated surfactant molecules and micelles – thus an equilibrium constant can be calculated. For a very dilute solutions of nonionic surfactant, where charge effects are absent and the activities of the substances in the solution closely approach the formal concentration, the single equilibrium can be described the equilibrium constant ( $K_{eq}$ ) which is given by following equation:

$$K_{eq} = \frac{a_{micelles}}{a_{monomes}^n} = \frac{[S_n]}{[S]^n} \quad (3)$$

where  $a_{micelles}$  is the activity of the spherical micelles and  $a_{monomers}$  is the activity of the monomeric surfactant molecules. The standard free energy change of micellization which is actually the reaction Gibbs energy change of micelle formation ( $\Delta_{mic}G^0$ ) can be expressed using Equation 4.

$$-\Delta_{mic}G^0 = -\frac{\Delta G}{n} = \frac{RT}{n} \ln K_{eq} = \frac{RT}{n} \ln [S_n] - RT \ln [S] \quad (4)$$

For the most surfactant systems,  $n > 50$  in this way the first term on the right-hand side of Equation (4) could be ignored. After simplification, the  $(\Delta_{mic}G^0)$  is given by:

$$\Delta_{mic}G^0 = RT\ln[S] = RT\ln[cmc] \quad (5)$$

which matches the appropriate result of the phase-separation model [19]. The close action model tolerates a simple extension to be made to the case of ionic surfactants, in which micelles attract a substantial proportion of counter ions, into an attached layer [20].

The thermodynamics of micellization can be determined from the study of the temperature-dependence of the CMC. For aqueous solutions of ionic and nonionic surfactants, the plots of CMC vs. temperature are usually U-shaped with a minimum at a characteristic temperature, generally around room temperature. The function of the temperature-dependence of the CMC can be described by either a polynomial equation or an equation in which case the analytical form is fully consistent with the van't Hoff equation. Furthermore, the variation of the natural logarithm of the CMC as a function of  $T$  can be approximated by a second-order polynomial [21].

$$\ln CMC = a + bT + cT^2 \quad (6)$$

Herein, CMC is expressed in mole fraction units and  $a$ ,  $b$  and  $c$  are the fitting constants. At a constant external pressure ( $P$ ), the isosteric enthalpy of micelle formation ( $\Delta_{mic}H_{vh}$ ) for non-ionic surfactants can be calculated by means of the van't Hoff relation [22].

$$\Delta_{mic}H_{vh} = -RT^2 \left( \frac{\partial \ln CMC}{\partial T} \right)_P \quad (7)$$

Furthermore, the entropy term ( $T\Delta_{mic}S$ ) and the heat capacity change ( $\Delta_{mic}C_p$ ) of micellization can also be given by the following equations [23, 24].

$$T\Delta_{mic}S = \Delta_{mic}H - \Delta_{mic}G \quad (8)$$

$$\Delta_{mic}C_p = \left( \frac{\partial (\Delta_{mic}H)}{\partial T} \right)_P \quad (9)$$

Additionally, besides the above described van't Hoff analysis the calorimetry is also a powerful method to obtain information directly on the enthalpy of micelle formation. Numerous researchers have reported on the enthalpy of micelle formation of single surfactant systems obtained by calorimetry [22] as well as there are some calorimetry studies on the micelle formation of surfactants in mixed solvent [25] or in the presence of cosurfactant [26]. By contrast, only a few studies demonstrate the enthalpy of mixed micelle formation obtained by calorimetry [27].

Beyond the above described theories and experimental evidences of micelle formation, the interactions between two surfactants in a mixed monolayer at the air/aqueous solution interface or their interaction in a mixed micelle in the aqueous phase play an important aspects for the detailed knowledge of the equilibrium properties of the self-assembly surfactant-based associated colloids [28]. Synergistic interactions between the surfactants in binary mixed systems can be predicted by some theories. There are common models used to describe the interactions and they are classified as the ideal and non-ideal representations. In the case of ideal solution theory (IST) which describes the mixing of the surfactants, the phase separation model can be used to calculate the CMC of the mixture ( $cmc_{mix}$ ) from the individual CMC,  $CMC_1$ , and  $CMC_2$ , and the respective mole fractions of surfactants ( $\alpha$ ). Based on the theoretical work by Clint [10] the  $CMC_m$  can be calculated using the following fundamental equation.

$$\frac{1}{cmc_m} = \frac{\alpha_1}{cmc_1} + \frac{\alpha_2}{cmc_2} \quad (10)$$

The non-ideal model creates the opportunity to calculate the extent of synergistic interaction provided by Rubingh [29]. A non-ideality parameter ( $\beta$ ) is required in the RST description of a binary system. Rubingh's treatment considers the activity coefficients given by the RST:

$$\ln f_1 = \beta(1 - X_1)^2 \quad (11)$$

$$\ln f_2 = \beta X_1^2 \quad (12)$$

where  $f_1$  and  $f_2$  are activity coefficients of the mixed surfactants,  $X_1$  is mole fraction of surfactant 1 in mixed micelle and  $\beta$  is the molecular interaction parameter, which takes into

account the interaction energy between the monomers of surfactant 1, surfactant 2, and monomers of surfactants 1 and 2 in the mixed micelle, respectively.

$$\beta^m = \frac{E_{11} + E_{22} - E_{12}}{RT} \quad (13)$$

Based on the phase separation model with ideal behavior of surfactants in the mixed micelle the surfactant concentrations in solution can be expressed using the individual and mixed CMC for the mixture and mole fraction of surfactants in mixed micelles and solution phase [30].

$$C_1 = X_1 cmc_1 f_1 = \alpha_1 cmc_m \quad (14)$$

$$C_2 = (1 - X_1) cmc_2 f_2 = (1 - \alpha_1) cmc_m \quad (15)$$

Equation 16, easily derived based on Equations (11, 12, 14 and 15), can be solved by an iterative calculation method that gives the mixed micelle composition ( $X_l$ ) from the experimental value of the  $CMC_m$ .

$$\frac{X_1^2 \ln\left(\frac{\alpha_1 cmc_m}{X_1 cmc_1}\right)}{(1 - X_1)^2 \ln\left(\frac{(1 - \alpha_1) cmc_m}{(1 - X_1) cmc_2}\right)} = 1 \quad (16)$$

The molecular interaction parameter for micelles ( $\beta^M$ ) can be evaluated using the equations (14 and 17). Hence, the  $\beta^M$  is given as:

$$\beta^M = \frac{\ln\left(\frac{\alpha_1 cmc_m}{X_1 cmc_1}\right)}{(1 - X_1)^2} \quad (17)$$

The nature and strength of the interaction between the surfactants are characterized by the value of the  $\beta^M$  parameter, which indicates the degree of non-ideality of the interaction in a mixed micelle. Based on the above defined relations, RST is able to describe clearly the interactions occurring in the mixed surfactant systems. Negative value of  $\beta^M$  indicates the synergistic nature of the interactions between these surfactants [31] while positive value of  $\beta^M$  signifies antagonism between components of surfactant combination [32].

## Experiment methods

### Chemicals

Nonionic surfactants (nonaethylene glycol mono(p-octylphenyl)ether/Lutensol<sup>®</sup> AP9 and icosaeethylene glycol mono(p-octylphenyl) ether/Lutensol<sup>®</sup> AP20) (**Figure S1**) were purchased from BASF Hungary Ltd. The surfactant solutions and their equimolar mixture-containing solutions were prepared in a 100 mL volumetric flask and then diluted in deionized water (18 MΩ cm<sup>-1</sup>, Milli Q, Millipore) to the desired concentration. All the starting materials were used without further purification.

### Surface tension measurements

The surface tension measurements of surfactant solutions were performed on a K100 MK2 Tensiometer (Krüss Co., Germany) using the Wilhelmy ring method in the concentration range of 4.5 mM – 4.5 μM using different compositions ( $0 < \alpha_I < 1$ ) as well. Before each measurement, the plate was carefully cleaned with deionized water and flamed. The surface tension of deionized water was measured to calibrate the tensiometer and to check the cleanliness of the sample pool. At a constant temperature and composition, the surface tension was measured at different concentrations by placing 50 mL volume of stock surfactant solution in sample pool and diluting with deionized water from a connected Dosimat 765 (Metrohm) titration stand. The solutions were immersed in a constant-temperature bath at the desired temperature (0.02 °C). Sets of measurements were taken at certain intervals until the surface tension was constant for 3 min. The standard deviation for surface tension measurements was less than 0.1 mN/m. Each measurement was performed at 288.15, 298.15, 308.15 and 318.15 K. During the automatized surface tension measurements the tensiometer and the dosing unit was controlled by the modularly constructed LabDesk<sup>™</sup> software.

### Isotherm titration calorimetry

Thermometric titration experiments were performed at 288.15 K with a computer-controlled VP-ITC power-compensation microcalorimeter (MicroCal). Deionized water (1.1 mL) in the sample cell was titrated under constant stirring with 300 μL of concentrated surfactant solution in aliquots of 10 μL in periodic time intervals of 5 min. The heat evolved or absorbed during the stepwise dilution experiment was recorded in the form of a series of



calorimeter peaks. The enthalpograms (calorimeter power signal vs time) were evaluated by means of Origin Microcal 7.1. software.

## Results and discussion

Surface tension values of the aqueous solutions of AP9 ( $\alpha_I = 1$ ) and AP20 ( $\alpha_I = 0$ ) and their mixtures ( $\alpha_I = 0.2$ ,  $\alpha_I = 0.4$ ,  $\alpha_I = 0.6$  and  $\alpha_I = 0.8$ ) are plotted against the logarithm of the total surfactant concentration at 298.15 K; the results are presented in **Figure 1**. As can be clearly seen, there are two linear intervals of the curves, connected by a short curved section. There are indications of negative deviations from linearity at the lowest concentrations, while the horizontal portion of the surface tension curves often had a minor positive slope. In spite of the mentioned nonlinearity, clear breaks can be observed in these curves which correspond to the individual CMC. Furthermore, the shape of curves is similar for both surfactants and their mixtures a linear dependence exists between interfacial tension and  $\ln C$  near the CMC. In the case of single surfactants ( $\alpha_I = 1$  and  $\alpha_I = 0$ ) the value of CMC agrees well with former experimental studies of micellization of polyethylene glycol mono(p-octylphenyl)ether type surfactants [33]. The interfacial tensions gradually decrease in the increasing analytical concentration of the surfactant until the air/solution interface becomes saturated with the surfactant where the micelle formation occurs. After complete interfacial saturation the  $\gamma$  vs.  $\ln C$  function remains nearly unchanged. The break points of the  $\gamma$  vs.  $\ln C$  curves were determined by linear regression founded routine via fitting of the both decreasing and the nearly horizontal portions of the curves (presented with gray dashed lines on **Figure 1** only for the pure AP20 (●)). The determined CMC value of the AP20 solution as a result of fitting is presented in **Figure 1** with black dashed line. For each sample, similar evaluation was performed. Based on the uncertainty of the slope and the intercept of a least squares fitted straight lines [34] as well as the basic rules of uncertainty calculations [35] the standard deviations of the CMC values can be easily determined. The CMC values of the investigated surfactants and their mixtures ( $\alpha_I = 0.2$ ; 0.4; 0.6; 0.8) with the corresponding standard deviations at different temperatures are presented in **Table 1**.

The experimentally determined CMC values of the mixed surfactants as a function of  $\alpha_I$  (**Figure 2**) show differences from the predicted values of ideal mixing based on equation (10) when the AP9 mole fraction is smaller than 0.5. As it can be seen on **Figure 2** in the range of  $\alpha_I = 1.0$ -0.8 the measured CMC values are similar to the predicted values calculated by the IST. The existence of non-ideal behavior is evident upon analysis of the data

summarized in **Table 1**, based on the difference ( $\Delta cmc$ ) between the calculated ( $cmc_{ideal}$ ) and the experimental ( $cmc_{exp}$ ) CMC values ( $\Delta cmc = cmc_{ideal} - cmc_{exp}$ ). The **Figure 3** visualizes the temperature- and composition- ( $\alpha_1$ ) dependence of  $\Delta cmc$ . We can conclude that measurable deviations from ideal behavior are observed over the entire investigated temperature and mole fraction range. As seen in **Figure 3** the maximum  $\Delta cmc$  is established at 288.15 K and at  $\alpha_1 = 0.2$ .

Moreover, the CMC values determined by surface tension shows the typical temperature-dependence which is presented in **Figure S2**. In many cases, the CMC of nonionic surfactants decrease as the temperature is increased. This is due to destruction of hydrogen bonds between water molecules and the hydrophilic headgroups. In this way, the CMC vs.  $T$  plot is nearly linear. Similar to the different studies of the temperature-dependence of CMC published previously for polyoxyethylenated non-ionic surfactant derivatives [36] our result also shows a slight nonlinearity; there is a minimum of the CMC-temperature curve in aqueous solution. As can be clearly seen, the CMC vs.  $T$  plots show the minimum at 298.15 K which was observed for both single surfactant as well as their mixtures. Besides the experimental CMC data, **Figure S2** shows the CMC predicted from equation (10).

According to the van't Hoff analysis, the natural logarithm of the CMC values were plotted against the absolute temperature as presented in **Figure 4**. As **Figure 4** shows the characteristics of  $\ln cmc$  – temperature data pairs can be described as a convex curve. The enthalpy change of micelle formation were obtained by a Microsoft Excel based nonlinear regression analysis [37] using equation (7). This procedure can determine the values for the parameters (a, b and c) of the second-order polynomial [equation (6)] by the minimalization the residual sum of squares of the distances of the experimental data points to the curve for the equation. The results of the nonlinear regression for each mole fraction are presented as dashed lines beside the experimental data of AP9 (♦), AP20 (●) in **Figure 4**.

Besides the calculated values of enthalpy by nonlinear parameter estimation, the uncertainty of the thermodynamic data is also important. To calculate the standard deviations of the fitting parameters, a weighted resampling “jackknife” procedure was used [38, 39]. Nonlinear parameter estimation-based fitting of the experimental data pairs (4 different  $\ln cmc$  vs.  $T$  data pairs) was repeated four times using different starting conditions. In the first case, all the data pairs were used for the calculation resulting in the mean value of the fitting parameters. For second run, the first data pair was neglected, while for third case the second data pairs was neglected and so on. After these procedure the standard deviation of the

pending parameters were calculable based on the recognized four different parameter set. The nonlinear parameter estimation-calculated van't Hoff enthalpies (in kJ mol<sup>-1</sup>) of micelle formation and the values of "jackknife" resampling technique evaluated standard deviations are listed in **Table 1**.

**Figure S3** shows that  $\Delta_{mic}H$  is reduced by raising the temperature. As a result,  $\Delta_{mic}H$  goes from positive to negative in the range 295-300 K in the case of single OPE (AP9 :  $\alpha_I = 1$  and AP20 :  $\alpha_I = 0$ ) and their mixtures ( $\alpha_I = 0.2$ ,  $\alpha_I = 0.4$ ,  $\alpha_I = 0.6$  and  $\alpha_I = 0.8$ ), thus the micelle formation changes from endothermic to exothermic at about 298 K. Before the inversion, the process is entropy-driven ( $T\Delta_{mic}S > 0$  and  $\Delta_{mic}H > 0$ ), but after inversion, both the entropy and enthalpy terms favor micelle formation ( $T\Delta_{mic}S > 0$  and  $\Delta_{mic}H < 0$ ). Linear extrapolations suggest that micellization becomes purely enthalpy-driven ( $T\Delta_{mic}S < 0$  and  $\Delta_{mic}H < 0$ ) above 340 K. Furthermore, there is a minimum in  $\Delta_{mic}H$  when the mole fraction of AP9 in the bulk phase is equal to 0.2. This nonlinear tendency of  $\Delta_{mic}H$  vs.  $\alpha_I$  plots and a minimum at  $\alpha_I = 0.2$  is unambiguously noticeable in the case of all the examined temperatures. According to simple algebraic calculations, the difference of the evaluated  $\Delta_{mic}H$  from the ideal behavior-predicted values increases as the temperature rising from 288.15 to 318.15 K and based on the value of determination coefficient ( $R^2 = 0.9974$  at  $\alpha_I = 0.2$ ) the relationship between the degree of the difference and T is almost completely linear.

In addition to the surface tension measurement based investigations at 288.15 K, the CMC and  $\Delta_{mic}H$  values were determined by isotherm titration calorimetry (ITC). The typical experimental titration curves obtained for the dilution of aqueous solutions of AP9 ( $\alpha_I = 1$ ) and AP20 ( $\alpha_I = 0$ ) into water are given in **Figure 5**. Moreover the single surfactants their mixtures ( $\alpha_I = 0.2$ ,  $\alpha_I = 0.4$ ,  $\alpha_I = 0.6$  and  $\alpha_I = 0.8$ ) were also examined via ITC technique, their thermograms and calorimetric enthalpies are not presented here. At the applied temperature the micellization process was exothermic for both the single surfactants and their mixtures equally. Taking into consideration the fact that the regular sigmoidal character is strongly distorted in both the premicellar and postmicellar regions the CMC and  $\Delta_{mic}H$  values were determined by a modified version of the sigmoidal Boltzman equation [23, 40]. The mentioned parameters and their standard deviations are presented in **Table 1**. Based on the ITC measurements we found that at 288.15 K the calorimetric enthalpies of micellization agree well with the van't Hoff enthalpies.

At the second stage of the evaluation process, the mixed micelle composition ( $X_I$ ) was determined from the experimental value of the  $CMC_m$  based on equation (16) which can be solved iteratively [41] to obtain the value of  $X_I$ . After determination of the  $X_I$ , the non-ideality

parameter ( $\beta^M$ ) which characterizes the nature and strength of the interaction between the surfactants can be calculated using Equation (17); the appropriate  $X_I$  and  $\beta^M$  values are presented in **Table 2**. As **Table 2** shows, all of the  $\beta^M$  values are negative, which indicates the appearance of a possible synergistic effect. To further verify the synergism the data summarized in Table 1 and in Table 3 should be analyzed according to the condition  $|\beta^M| > |\ln(\text{cmc}_1/\text{cmc}_2)|$ . The value of the calculated  $\beta^M$  parameters for all the investigated mixtures are smaller than the required level which leads to the conclusion that our binary surfactant system does not fulfill the second condition of the existence of synergism. Meanwhile, the deviation from the ideal behavior is observed from all the investigated temperatures and mole fraction ranges taking into account the negative sign of  $\beta^M$  parameters. According the composition- ( $\alpha_I$ ) and temperature-dependence of  $\beta^M$  results were found as in the case of the evolution of  $\Delta_{mic}H$  in the mole fraction-, temperature- and enthalpy-determined three dimensional parameter space. Namely, viewing the system from the aspect of composition the value of  $\beta^M$  takes a minimum when the mole fraction of AP9 in the bulk phase is equal 0.2. This type of minimum curve is noticeable the whole investigated temperature range. Values of  $\beta^M$  increase as the temperature increases from 288.15 to 318.15 K and the relationship between  $\beta^M$  and T is almost fully linear.

As final outcomes of the investigation of the mixed micelle formation we compared the evolution of the experimentally CMC<sub>m</sub>-based Gibbs free energy ( $\Delta_{mic}G_m$ ), the IST-based ( $\Delta_{mic}G_{ideal}$ ) and the RST-predicted excess Gibbs free energy ( $G^E$ ) [42, 43]. Firstly, we calculated the  $\Delta_{mic}G_m$  values using equation (5), the  $\Delta_{mic}G_{ideal}$  values by equation (13) analogously and composed the difference of this data pairs ( $\Delta_{mic}G_m - \Delta_{mic}G_{ideal}$ ). The absolute values of these differences were plotted against the molar ratio of surfactant mixture ( $\alpha_I$ ) in the case of the four different temperature can be seen in **Figure 6**. Besides the previously mentioned differences which characterize the degree of non-ideal behavior, the  $G^E$  were also calculated and the values are represented on **Figure 6** as well.  $G^E$  were calculated as linear functions of the mixed micelle composition ( $X_I$ ) and activity coefficients of the mixed surfactants ( $f_1$  and  $f_2$ ) according to  $G^E = RT(X_I \ln f_1 + X_2 \ln f_2)$  expression. In this manner, the various calculations were successfully applied in order to determine the excess properties of mixed surfactants in the mixed micelles. In **Figure 6**, the difference of experimental cmc<sub>m</sub> based ( $\Delta_{mic}G_m$ ) and IST predicted ( $\Delta_{mic}G_{ideal}$ ) Gibbs free energy is symbolized by full-, while the RST based excess Gibbs free energy ( $G^E$ ) represented as hollow symbols. Dotted lines are drawn to guide the eye. As can be seen on **Figure 6** analogous trends were observed for both approximation originated excess quantities. A deeper interpretation of this result provides the

existence of a nearly synergistic interaction which can be characterized by well-defined excess Gibbs free energy.

## Conclusions

Based on the tensiometric profile of the aqueous solutions of AP9 and AP20 surfactants and their mixtures, the CMC values and the corresponding standard deviations were determined at different temperatures and compositions. In the investigated temperature (288.15 – 318.15 K) and bulk mole fractions (from 0.0 up to 1.0 for AP9) range we found that the CMC values are lower than  $CMC_{ideal}$  calculated from ideal mixing model. The CMC versus T curve of single and mixed surfactants passes through a minimum just below room temperature. Results of the nonlinear regression analysis showed that  $\Delta_{mic}H$  is reduced upon raising the temperature and there is a minimum of the  $\Delta_{mic}H$  when the mole fraction of AP9 in the bulk phase is equal to 0.2. The calorimetric enthalpies of micelle formation agreed well with the enthalpies calculated via the van't Hoff relation. The Gibbs free energy of single and mixed micelle formation was nearly constant as the temperature was increased, due to enthalpy/entropy compensation. Comparison of the experimentally, IST-based and the RST-predicted excess Gibbs free energy resulted in similar trends for both approximation initiated excess quantities which provides the presence of a synergistic type interaction.

## Acknowledgement

The research was supported by National Research, Development and Innovation Office-NKFIH through project "Synthesis, structural and thermodynamic characterization of nanohybrid systems at solid-liquid interfaces" K116323, GINOP-2.3.2-15-2016-00013 and GINOP-2.3.2-15-2016-00060. The authors are grateful to Szilárd Ocskó MSc student (University of Szeged, Department of Physical Chemistry and Materials Sciences) for help in carrying out the surface tension measurements. Edit Csapó gratefully acknowledges the financial support of J. Bolyai Research Fellowship of the Hungarian Academy of Sciences.

## References

1. Kulthe SS, Inamdar NN, Choudhari YM, et al (2011) Mixed micelle formation with hydrophobic and hydrophilic Pluronic block copolymers: Implications for controlled and targeted drug delivery. *Colloids Surfaces B Biointerfaces* 88:691–696. doi: 10.1016/j.colsurfb.2011.08.002
2. Qian C, Decker EA, Xiao H, McClements DJ (2012) Nanoemulsion delivery systems: Influence of carrier oil on  $\beta$ -carotene bioaccessibility. *Food Chem* 135:1440–1447. doi: 10.1016/j.foodchem.2012.06.047
3. Rao J, McClements DJ (2012) Lemon oil solubilization in mixed surfactant solutions: Rationalizing microemulsion & nanoemulsion formation. *Food Hydrocoll* 26:268–276. doi: 10.1016/j.foodhyd.2011.06.002
4. Faustino CMC, Serafim CS, Ferreira IN, et al (2014) Mixed Micelle Formation between an Amino Acid-Based Anionic Gemini Surfactant and Bile Salts. *Ind Eng Chem Res* 53:10112–10118. doi: 10.1021/ie5003735
5. Rathman JF (1996) Micellar catalysis. *Curr Opin Colloid Interface Sci* 1:514–518. doi: 10.1016/S1359-0294(96)80120-8
6. Poša M, Popović K, Ćirin D, Agatić ZF (2016) Binary mixed micelles of triton X-100 and selected bile salts: Thermodynamic stabilization and pKa values of micellar bile acids. *J Chem Thermodyn* 103:333–341. doi: 10.1016/j.jct.2016.08.030
7. Poša M, Pilipović A, Bećarević M, Farkaš Z (2017) pKa values of hyodeoxycholic and cholic acids in the binary mixed micelles sodium-hyodeoxycholate–Tween 40 and sodium-cholate–Tween 40: Thermodynamic stability of the micelle and the cooperative hydrogen bond formation with the steroid skeleton. *Steroids* 117:62–70. doi: 10.1016/j.steroids.2016.09.012
8. Hoffmann H, Poessnecker G (1994) The Mixing Behavior of Surfactants. *Langmuir* 10:381–389. doi: 10.1021/la00014a009
9. Holland PM (1986) Nonideal mixed micellar solutions. *Adv Colloid Interface Sci* 26:111–129. doi: 10.1016/0001-8686(86)80018-5
10. Clint JH (1975) Micellization of mixed nonionic surface active agents. *J Chem Soc Faraday Trans 1 Phys Chem Condens Phases* 71:1327. doi: 10.1039/f19757101327



11. Moroi Y (1992) Mixed Micelle Formation. In: Micelles. Springer US, Boston, MA, pp 183–194
12. Motomura K, Yamanaka M, Aratono M (1984) Thermodynamic consideration of the mixed micelle of surfactants. *Colloid Polym Sci* 262:948–955. doi: 10.1007/BF01490027
13. Corkill JM, Goodman JF, Harrold SP (1964) Thermodynamics of micellization of non-ionic detergents. *Trans Faraday Soc* 60:202. doi: 10.1039/tf9646000202
14. Hildebrand A, Garidel P, Neubert R, Blume A (2004) Thermodynamics of Demicellization of Mixed Micelles Composed of Sodium Oleate and Bile Salts. *Langmuir* 20:320–328. doi: 10.1021/la035526m
15. Szymczyk K, Jańczuk B (2007) The adsorption at solution–air interface and volumetric properties of mixtures of cationic and nonionic surfactants. *Colloids Surfaces A Physicochem Eng Asp* 293:39–50. doi: 10.1016/j.colsurfa.2006.07.006
16. Schreier S, Malheiros SVP, de Paula E (2000) Surface active drugs: self-association and interaction with membranes and surfactants. *Physicochemical and biological aspects. Biochim Biophys Acta - Biomembr* 1508:210–234. doi: 10.1016/S0304-4157(00)00012-5
17. Elias H-G (1973) Nonionic Micelles. *J Macromol Sci Part A - Chem* 7:601–622. doi: 10.1080/00222337308061161
18. Stasiuk ENB, Schramm LL (1996) The Temperature Dependence of the Critical Micelle Concentrations of Foam-Forming Surfactants. *J Colloid Interface Sci* 178:324–333. doi: 10.1006/jcis.1996.0120
19. Corkill JM, Goodman JF, Harrold SP (1964) Thermodynamics of micellization of non-ionic detergents. *Trans Faraday Soc* 60:202. doi: 10.1039/tf9646000202
20. Phillips JN (1955) The energetics of micelle formation. *Trans Faraday Soc* 51:561. doi: 10.1039/tf9555100561
21. Nusselder JJH, Engberts JBF. (1992) Toward a better understanding of the driving force for micelle formation and micellar growth. *J Colloid Interface Sci* 148:353–361. doi: 10.1016/0021-9797(92)90174-K

22. Chatterjee A, Moulik SP, Sanyal SK, et al (2001) Thermodynamics of micelle formation of ionic surfactants: A critical assessment for sodium dodecyl sulfate, cetyl pyridinium chloride and dioctyl sulfosuccinate (Na salt) by microcalorimetric, conductometric, and tensiometric measurements. *J Phys Chem B* 105:12823–12831. doi: 10.1021/jp0123029
23. Páhi AB, Király Z, Mastalir Á, et al (2008) Thermodynamics of Micelle Formation of the Counterion Coupled Gemini Surfactant Bis(4-(2-dodecyl)benzenesulfonate)-Jeffamine Salt and Its Dynamic Adsorption on Sandstone. *J Phys Chem B* 112:15320–15326. doi: 10.1021/jp806522h
24. Muller N (1993) Temperature dependence of critical micelle concentrations and heat capacities of micellization for ionic surfactants. *Langmuir* 9:96–100. doi: 10.1021/la00025a022
25. Callaghan A, Doyle R, Alexander E, Palepu R (1993) Thermodynamic properties of micellization and adsorption and electrochemical studies of hexadecylpyridinium bromide in binary mixtures of 1,2-ethanediol with water. *Langmuir* 9:3422–3426. doi: 10.1021/la00036a016
26. Landry JM, Marangoni DG (2008) The effect of added alcohols on the micellization process of sodium 8-phenyloctanoate. *Colloid Polym Sci* 286:655–662. doi: 10.1007/s00396-007-1809-3
27. Ohta A, Miyagishi S, Aratono M (2001) Calorimetry of Micelle Formation of Binary Nonionic Surfactant Mixtures. *Society* 2277:2826–2832. doi: 10.1021/jp003521h
28. Rosen MJ, Zhou Q (2001) Surfactant–Surfactant Interactions in Mixed Monolayer and Mixed Micelle Formation. *Langmuir* 17:3532–3537. doi: 10.1021/la001197b
29. Holland PM, Rubingh DN (1983) Nonideal multicomponent mixed micelle model. *J Phys Chem* 87:1984–1990. doi: 10.1021/j100234a030
30. Elvira Rodenas \*, Mercedes Valiente, and Ma del Sol Villafruela (1999) Different Theoretical Approaches for the Study of the Mixed Tetraethylene Glycol Mono-n-dodecyl Ether/Hexadecyltrimethylammonium Bromide Micelles. *J Phys Chem B* 103:4549–4554. doi: 10.1021/jp981871m
31. Szymczyk K, Janczuk B (2007) The Properties of a Binary Mixture of Nonionic



- Surfactants in Water at the Water / Air Interface. *Langmuir* 23:4972–4981. doi: 10.1021/LA063554+
32. Kamil M, Siddiqui H (2013) Experimental Study of Surface and Solution Properties of Gemini -conventional Surfactant Mixtures on Solubilization of Polycyclic Aromatic Hydrocarbon. *Model Numer Simul Mater Sci* 3:17–25. doi: 10.4236/mnsms.2013.34B004
33. Hsiao L, Dunning HN, Lorenz PB (1956) Critical Micelle Concentrations of Polyoxyethylated Non-ionic Detergents. *J Phys Chem* 60:657–660. doi: 10.1021/j150539a037
34. York D, Evensen NM, Martínez MLL, De Basabe Delgado JJ (2004) Unified equations for the slope, intercept, and standard errors of the best straight line. *Am J Phys* 72:367. doi: 10.1119/1.1632486
35. Farrance I, Frenkel R (2012) Uncertainty of Measurement: A Review of the Rules for Calculating Uncertainty Components through Functional Relationships. *Clin Biochem Rev* 33:49–75.
36. Chen L-J, Lin S-Y, Huang C-C, Chen E-M (1998) Temperature dependence of critical micelle concentration of polyoxyethylenated non-ionic surfactants. *Colloids Surfaces A Physicochem Eng Asp* 135:175–181. doi: 10.1016/S0927-7757(97)00238-0
37. Juhász Á, Csapó E, Ungor D, et al (2016) Kinetic and Thermodynamic Evaluation of Kynurenine Acid Binding to GluR1<sub>270–300</sub> Polypeptide by Surface Plasmon Resonance Experiments. *J Phys Chem B* 120:7844–7850. doi: 10.1021/acs.jpcb.6b05682
38. Caceci MS (1989) Estimating error limits in parametric curve fitting. *Anal Chem* 61:2324–2327. doi: 10.1021/ac00195a023
39. Juhász Á, Csapó E, Vécsei L, Dékány I (2017) Modelling and Characterization of the Sorption of Kynurenine Acid on Protein Surfaces. *Period Polytech Chem Eng* 61:3–9. doi: 10.3311/PPCH.10185
40. Király Z, Dekány I (2001) A Thermometric Titration Study on the Micelle Formation of Sodium Decyl Sulfate in Water. *J Colloid Interface Sci* 242:214–219. doi: 10.1006/jcis.2001.7777
41. Vautier-Giongo C, Bakshi MS, Singh J, et al (2005) Effects of interactions on the

formation of mixed micelles of 1,2-diheptanoyl-sn-glycero-3-phosphocholine with sodium dodecyl sulfate and dodecyltrimethylammonium bromide. *J Colloid Interface Sci* 282:149–155. doi: 10.1016/j.jcis.2004.08.071

42. De Lisi R, Inglese A, Milioto S, Pellerito A (1996) Excess free energy, enthalpy and entropy of surfactant-surfactant mixed micelle formation. *Fluid Phase Equilib* 126:273–287. doi: 10.1016/S0378-3812(96)03100-7

43. Iyota H, Todoroki N, Ikeda N, et al (1998) Nonideal Mixing of Decyl Methyl Sulfoxide and Decyldimethylphosphine Oxide in Adsorbed Films and Micelles. *J Colloid Interface Sci* 208:203–210. doi: 10.1006/jcis.1998.5793

## Figure captions

**Fig. 1.** Representative equilibrium surface tension data of the aqueous solutions of AP9 (♦), AP20 (●) and their mixtures (unfilled symbols) close to  $cmc$  at 298.15 K. Mole fraction ( $\alpha_1$ ) data relate to the AP9.

**Fig. 2.**  $\Delta cmc$  data as a function of AP9 mole fraction ( $\alpha_1$ ) at 288.15 K (dotted line). The dashed grey line corresponds to the calculated  $cmc$  values according to IST [equation (10)].

**Fig. 3.**  $\Delta cmc$  data derived from IST predicted values ( $\Delta cmc = cmc_{ideal} - cmc_{exp}$ ) as a function of AP9 mole fraction ( $\alpha_1$ ) and temperature.

**Fig. 4.** Natural logarithm of  $cmc$  as a function of the temperature for single surfactants (AP9:  $\alpha_1 = 1$  and AP20:  $\alpha_1 = 0$ ). The dashed grey lines represent the fitting of the measured data via nonlinear regression fits based on equation (7).

**Fig. 5.** Typical thermograms and calorimetric enthalpies of dilution obtained from ITC experiments for single surfactants at 288.15 K. Results from a fit of the experimental data to the modified Boltzmann equation (solid lines).

**Fig. 6.** Different evaluation process resulted excess Gibbs free energy of mixed micelle formation as a function of composition ( $\alpha_1$ ) at different temperatures.

## Table captions

**Table 1.** Surface tension- and ITC measurement determined  $cmc$  and  $\Delta_{mic}H$  values of single (AP9:  $\alpha_1 = 1$  and AP20:  $\alpha_2 = 1$ ) and mixed ( $\alpha_1 = 0.2$ ,  $\alpha_1 = 0.4$ ,  $\alpha_1 = 0.6$  and  $\alpha_1 = 0.8$ ) surfactants at a different mole fractions ( $\alpha_1$ ) and temperatures.

**Table 2.** Calculated micelle compositions ( $X_1$ ) and molecular interactions parameters ( $\beta^M$ ) of the investigated surfactant mixtures at different mole fractions ( $\alpha_1$ ) and temperatures.

**Table captions**

**Table 1.** Surface tension- and ITC measurement determined CMC and  $\Delta_{mic}H$  values of single (AP9:  $\alpha_I = 1$  and AP20:  $\alpha_2 = 1$ ) and mixed ( $\alpha_I = 0.2$ ,  $\alpha_I = 0.4$ ,  $\alpha_I = 0.6$  and  $\alpha_I = 0.8$ ) surfactants at a different mole fractions ( $\alpha_I$ ) and temperatures.

**Table 2.** Calculated micelle compositions ( $X_I$ ) and molecular interactions parameters ( $\beta^M$ ) of the investigated surfactant mixtures at different mole fractions ( $\alpha_I$ ) and temperatures.

For Peer Review

**Table 1.**

<b>T (K)</b>	<b>mole fraction (<math>\alpha_1</math>)</b>					
	<b>1.0</b>	<b>0.8</b>	<b>0.6</b>	<b>0.4</b>	<b>0.2</b>	<b>0.0</b>
<b>288.15</b>	0.052±0.005	0.060±0.006	0.068±0.007	0.078±0.008	0.095±0.009	0.163±0.015
	0.066±0.005 <sup>#</sup>	0.062±0.005 <sup>#</sup>	0.080±0.004 <sup>#</sup>	0.068±0.005 <sup>#</sup>	0.092±0.003 <sup>#</sup>	0.186±0.022 <sup>#</sup>
<b>298.15</b>	0.048±0.004	0.055±0.005	0.063±0.006	0.074±0.007	0.093±0.008	0.157±0.014
<b>308.15</b>	0.053±0.005	0.061±0.006	0.071±0.007	0.083±0.008	0.105±0.009	0.170±0.015
<b>318.15</b>	0.062±0.006	0.071±0.007	0.084±0.008	0.102±0.010	0.132±0.011	0.201±0.018
<b>T (K)</b>	<b><math>\Delta_{\text{mic}}H</math> (kJ mol<sup>-1</sup>)</b>					
	<b>1.0</b>	<b>0.8</b>	<b>0.6</b>	<b>0.4</b>	<b>0.2</b>	<b>0.0</b>
<b>288.15</b>	8.51±1.52	7.98±1.54	7.13±1.28	6.30±1.13	4.85±0.90	5.78±1.36
	7.75±0.51 <sup>#</sup>	7.4±0.55 <sup>#</sup>	5.24±0.28 <sup>#</sup>	4.68±0.34 <sup>#</sup>	3.49±0.12 <sup>#</sup>	5.74±0.68 <sup>#</sup>
<b>298.15</b>	0.09±0.75	-0.32±0.75	-1.21±0.63	-2.32±0.39	-3.69±0.31	-1.47±0.13
<b>308.15</b>	-9.54±0.42	-9.91±0.42	-10.74±0.36	-12.15±1.47	-13.43±1.17	-9.75±0.47
<b>318.15</b>	-20.44±1.35	-20.71±1.39	-21.53±1.14	-23.27±2.94	-24.43±2.35	-19.12±2.35

<sup>#</sup> data determined by ITC studies

1  
2  
3  
4  
5  
6  
7  
8  
9  
10  
11  
12  
13  
14  
15  
16  
17  
18  
19  
20  
21  
22  
23  
24  
25  
26  
27  
28  
29  
30  
31  
32  
33  
34  
35  
36  
37  
38  
39  
40  
41  
42  
43  
44  
45  
46  
47  
48  
49  
50  
51  
52  
53  
54  
55  
56  
57  
58  
59  
60

Table 2.

$\alpha_1$	288.15 K		298.15 K		308.15 K		318.15 K	
	$X_1$	$\beta^M$	$X_1$	$\beta^M$	$X_1$	$\beta^M$	$X_1$	$\beta^M$
1.0	-	-	-	-	-	-	-	-
0.8	0.91	-0.23	0.92	-0.20	0.92	-0.10	0.92	-0.07
0.6	0.79	-0.39	0.80	-0.31	0.81	-0.22	0.82	-0.12
0.4	0.64	-0.57	0.66	-0.45	0.66	-0.36	0.67	-0.18
0.2	0.45	-0.78	0.46	-0.62	0.45	-0.46	0.45	-0.24
0.0	-	-	-	-	-	-	-	-

For Peer Review

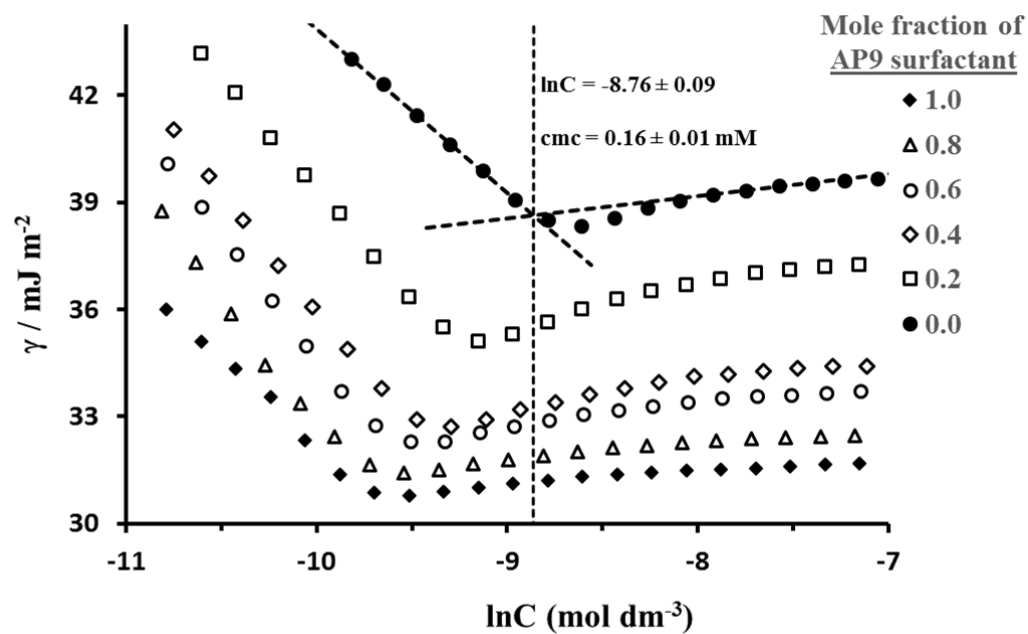


Figure 1.

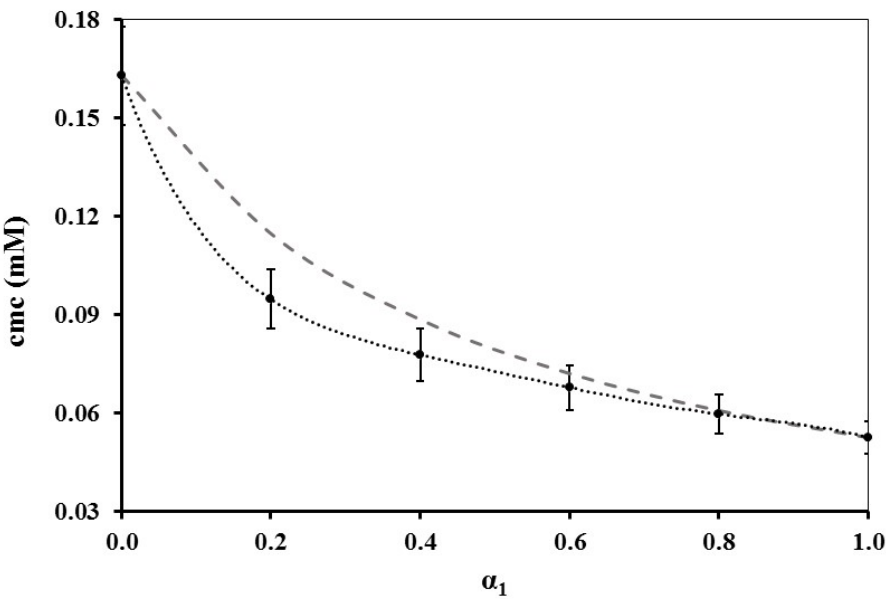


Figure 2.



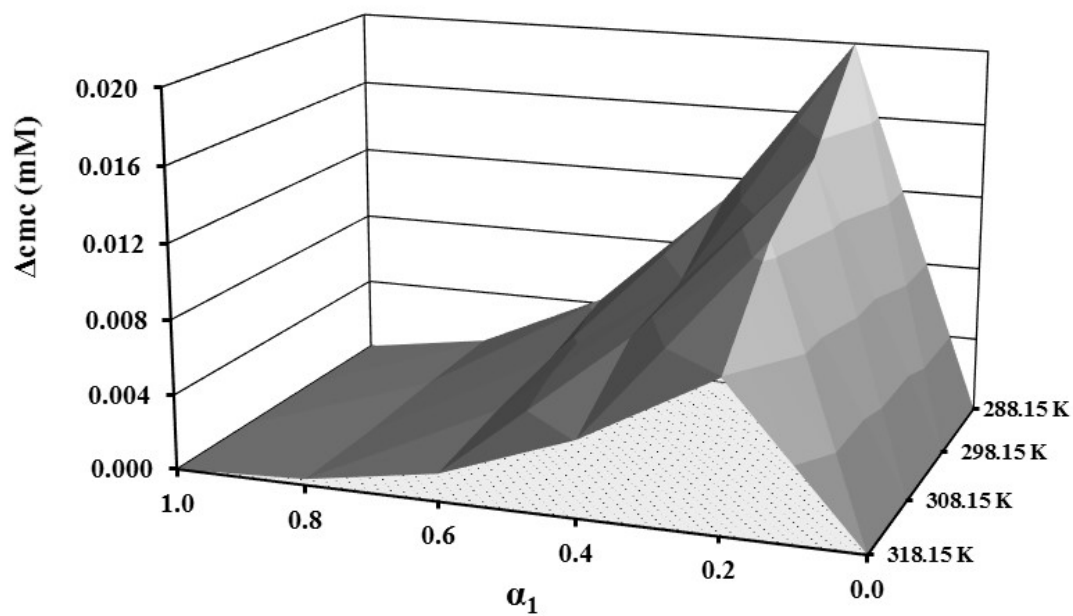


Figure 3.

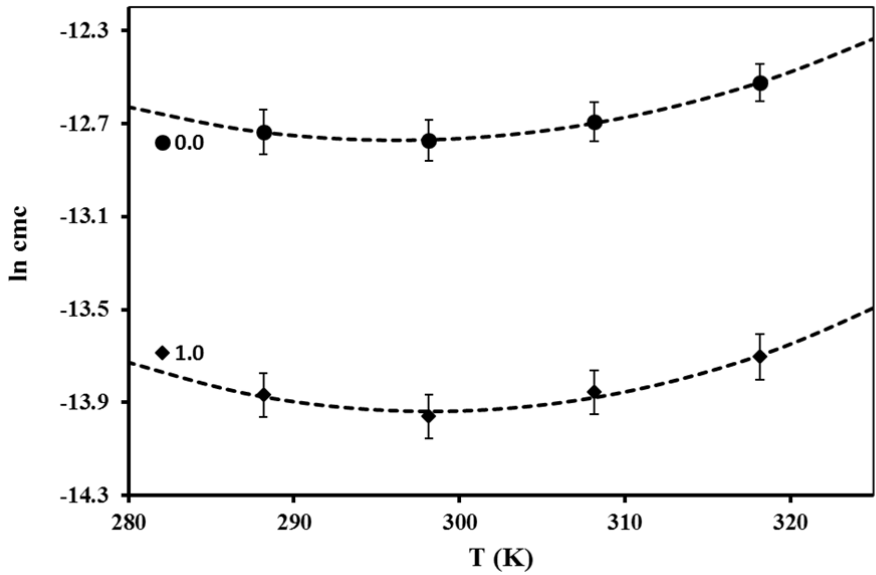


Figure 4.

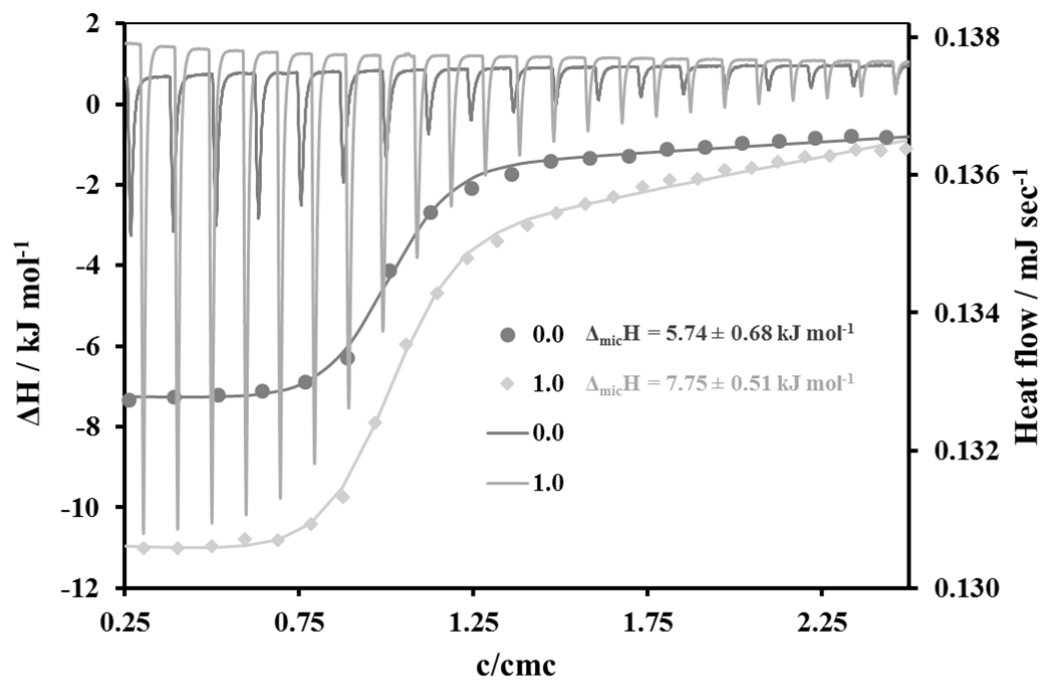


Figure 5.

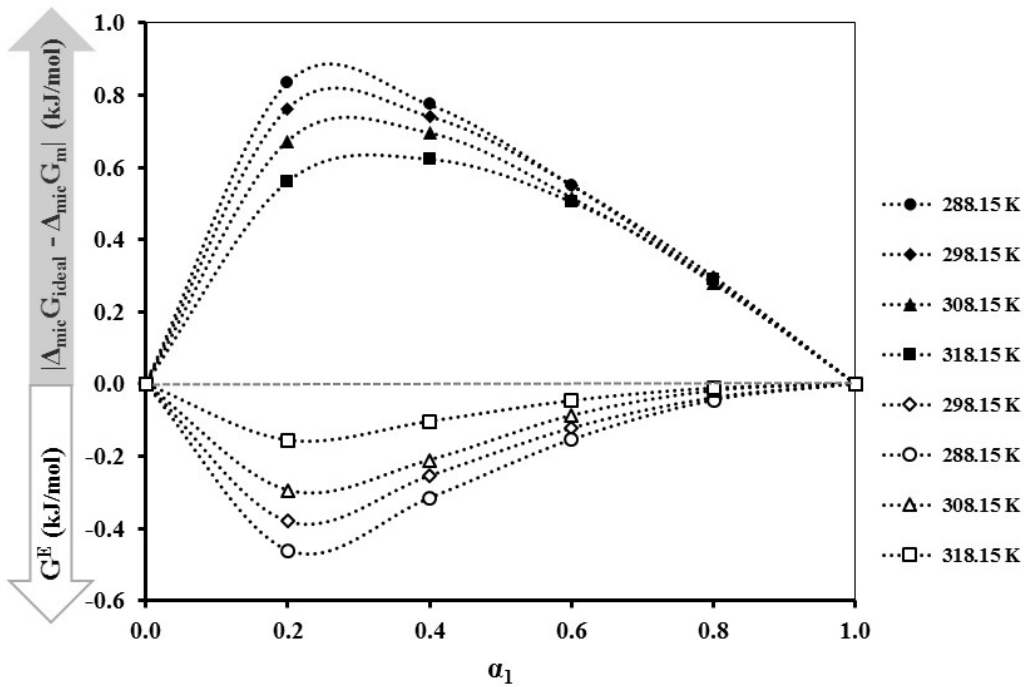


Figure 6.